Modeling of 3D Left Ventricular Motion to Evaluate Paced Myocardial Function

Dong Ni, Siping Chen, Hongmei Sun, Tianfu Wang*
Department of Biomedical Engineering, School of Medicine
Shenzhen University, Shenzhen, China

***Abstract*—Pacemaker is widely used to help control abnormal heart rhythms. In this paper, we propose to evaluate the paced myocardial function by building a Three-Dimensional (3D) mechanical motion model of Left Ventricular (LV), in order to optimize the pacing models. We first create a 3D standard LV model based on manually segmented LV segments by experienced clinicians. The mechanical motion of LV is further measured using Two-Dimensional (2D) Ultrasonic Doppler Tissue Velocity (DTV) imaging, and correlated with the 3D LV model by Mutual Information (MI) based non-rigid registration methods. Such multiple 2D motion images are then mapped to the 3D LV model by interpolation. The preliminary experiments are carried out by comparing the myocardial function before and after pacemaker implantation, and prove the promising feasibility of our proposed method.**

Keywords-Mechanical motion; Myocardium; Doppler tissue velocity; Pacemaker; Left ventricular; 3D model

I. INTRODUCTION

Cardiovascular disease is the leading cause of death in the world, due to the inability of the heart to fill with or pump out enough blood to meet the body's needs. Implanting artificial pacemakers is treated as an effective means to regulate the beating of the heart. Modern pacemakers are externally programmable and allow the cardiologists to select the optimum pacing modes for individual patients, which depends on the qualitative and quantitative evaluation of the individual's cardiac function.

Some research work focused on the analysis of hemodynamics. Kim et al. [1] proposed to quantify the short term hemodynamic effects of biventricular pacing in patients with heart failure by making use of 3D echocardiography. Kerwin et al. [2] evaluated the effects of biventricular pacing on contractile synchrony and ejection fraction based on phase image analysis. However, traditional hemodynamic can not measure the mechanical motion of the myocardium, which is truly important for the evaluation of the cardiac function.

Other research groups tried to evaluate the cardiac function by studying the cardiac-electrophysiology. Alonso et al. [3] compared the electrocardiogram of 29 patients with Biventricular pacemaker implanted. Rouleau et al. [4] defined the criteria for left ventricular pacing in dilated cardiomyopathy using an echocardiographic evaluation of interventricular electromechanical delay. Although cardiac-electrophysiology is useful for the routine diagnois of cardiac disease, it is relatively slow and inaccurate.

Recent studies showed the importance of analyzing the mechanical motion of myocardium [5] [6] [7]. Among them, Doppler Tissue Velocity (DTV) is widely used to measure the velocity of myocardial motion, as ultrasound imaging is cheap, harmless, and allows for real-time image acquisitions [6]. Moreover, LV motion model proved to be important for cardiovascular mechanical and dynamics evaluation [8].

In this paper we propose to build a 3D mechanical motion model of LV, in order to evaluate the cardiac function and thus help the optimization of pacing models (Figure 1). Firstly a 3D standard LV model is created by manual segmentation of LV segments by experienced clinicians. Then the myocardial motion of LV is measured by using 2D Ultrasonic DTV imaging. DTV images are further correlated with corresponding positions of the 3D LV model by Mutual Information (MI) based non-rigid registration methods and mapped to the 3D LV model. Finally, we compare the myocardial motion function of LV before and after pacemaker implantation.

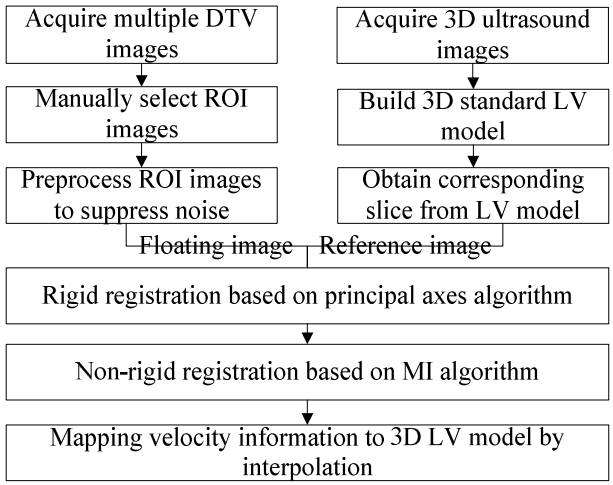

Figure 1. Flow diagram of proposed methods.

II. METHODS

A. Creation of 3D Standard LV Model

Standard LV model is important for the comparison of the myocardial motion function between different patients. But it is very difficult to build an accurate 3D standard LV by matching and averaging multiple models of different patients, because of the complicated anatomical structure of LV, the great difference between persons and the deformability of heart. We propose to apply the 16-segment biomechanical model of LV (Figure 2) to build the 3D standard LV model. This method has the merit of easy use and can eliminate the anatomical difference of LV between persons to some extent [9].

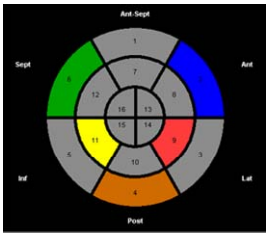

Figure 2. 16 segment biomechanical model of LV.

The 3D echocardiogram images of LV are first obtained by Philips Sonos 7500 echo system. Then 16 segments of LV are manually segmented from the slices of the 3D images by experienced cardiologists. Based on these segments, the triangularization and surface reconstruction methods used in [10] are applied to build the 3D standard LV model. Finally, the mesh filtering algorithms in [10] are used to make the surface smoother. Figure 3(a) displays the myocardium model in end-diastolic phase, and Figure 3(b) shows the myocardium model in end-systolic phase.

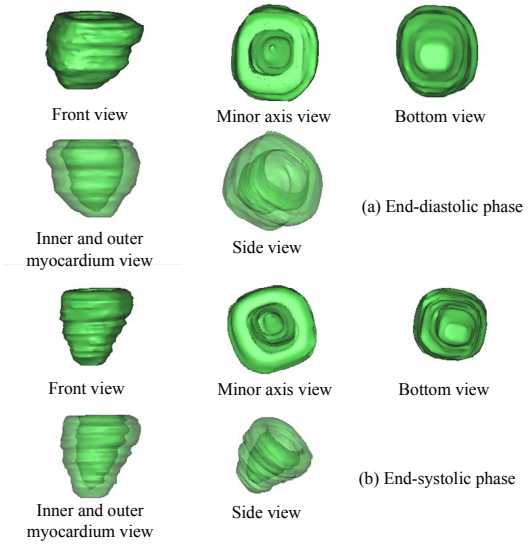

Figure 3. 3D standard LV models.

B. Registration of DTV Image and Standard LV Model

Motion analysis of LV has important clinical value for the assessment of cardiac function. Together with cardio-Magnetic Resonance Imaging (MRI), echocardiography is nowadays the reference modality to study the regional myocardial function in clinical practice. As one method of echocardiography, DTV imaging offers significant advantages over MRI since ultrasound imaging is real-time, radiation free and cheap. Moreover, DTV imaging can directly measure the motion of myocardium, while other motion analysis algorithms based on gray-level echocardiography have to detect features or track speckles, which is difficult and time-consuming for ultrasound data due to its poor signal-to-noise ratio [6].

The DTV images of LV are first acquired and filtered by using a well-known technique, e.g. by a Gaussian filter, in order to reduce the noise [11]. Because of the difference between individual DTV images and standard LV model, we propose a two-step method to match filtered DTV images with corresponding segments of 3D LV model by rigid registration methods based on principal axes algorithm, and further non-rigid registration methods using MI algorithm.

The principal axes algorithm can register the medical images rapidly and serve as the initial step of the following non-rigid registration [12]. Given a 2D image $f(m,n)$, the moment m_{pq} and central moment u_{pq} of the image are defined as:

$$m_{pq} = \sum_{m=1}^{M}\sum_{n=1}^{N} m^p n^q f(m,n) \tag{1}$$

$$u_{pq} = \sum_{m=1}^{M}\sum_{n=1}^{N} (m-\bar{x})(n-\bar{y}) f(m,n) \tag{2}$$

Where p and q are two orders of the moment and $(\bar{x},\bar{y})$ is the centroid of the image, defined as:

$$\bar{x} = m_{10}/m_{00} \qquad \bar{y} = m_{01}/m_{00} \tag{3}$$

The angle between the principle axis and y-axis is given as:

$$\tan 2\theta = 2\mu_{11}/(\mu_{20}-\mu_{02}) \tag{4}$$

Then the translation $(\Delta x, \Delta y)$ and the rotation angle $\Delta\theta$ are given as the difference of the centroids and the principle angles of the floating image and reference image.

Initialized by the transformation matrix obtained from the first step, MI algorithm, as a well-known registration method for medical images, is applied in the non-rigid registration step. Given the contours of the floating image and reference image as two sets of points $(X_i, i=1,2,...,N_1), (Y_j, j=1,2,...,N_2)$, the MI of two images is taken as:

$$MI(X,Y) = \sum_{i=1}^{N_1}\sum_{j=1}^{N_2} p_{ij} \log\left(p_{ij} \Big/ \sum_{k=1}^{N_1} p_{kj} \sum_{l=1}^{N_2} p_{il}\right) \tag{5}$$

$$p_{ij} = \exp(-\alpha D_{ij} - \lambda) \qquad D_{ij} = \| X_i - TY_j \| \tag{6}$$

Where α, λ are two constants selected by the user, and T is the deformation field. Then both the deformation field and MI value are optimized by Metropolis algorithm [13], which is kind of global optimization algorithm and proved to be robust for the medical image registration based on MI algorithm [14]. Such optimization procedure is stopped when the maximal MI value is found. At last, the floating image is transformed to the reference image using B-spline interpolation methods [15].

C. Mapping Velocity Information to LV Model

Once the correlation between 2D DTV images and 3D LV model is obtained, the velocity information can be mapped to the 3D LV model by interpolation. It is difficult to achieve the performance of both high speed and high accuracy at the same time for surface interpolation because of a large number of mesh cells included in the 3D LV model. In addition, the shape formed by four control points is not regular, which may slow down the interpolation speed. We adopted the fast bilinear interpolation algorithm [16] to the 3D LV model. Our method includes four steps:

(1) Given three orthogonal axis *x, y, z*, project the target point and the nearest four control points to Plane(*x, y*), Plane(*z, y*) and Plane(*x, z*) to get three irregular quadrilaterals and three projected target points.

(2) Map the irregular quadrilateral (*a, b, c, d*) to a rectangle (*a', b', c', d'*) (shown in Figure 4). One point *P(x, y)* located in the quadrilateral is given as:

$$\begin{aligned} x &= (1-\beta)(1-\alpha)a_x + (1-\beta)\alpha d_x + (1-\alpha)\beta b_x + \alpha\beta c_x \\ y &= (1-\beta)(1-\alpha)a_y + (1-\beta)\alpha d_y + (1-\alpha)\beta b_y + \alpha\beta c_y \end{aligned} \quad (7)$$

Where a_x, b_x, c_x and a_y, b_y, c_y are the coordinates of points *a, b, c,* and $0<\alpha<1, 0<\beta<1$. Parameters α and β can be calculated from equation (7). In like manner, the corresponding point $P(x', y')$ of *P(x, y)* is taken as:

$$\begin{aligned} x' &= (1-\beta)(1-\alpha)a'_x + (1-\beta)\alpha d'_x + (1-\alpha)\beta b'_x + \alpha\beta c'_x \\ y' &= (1-\beta)(1-\alpha)a'_y + (1-\beta)\alpha d'_y + (1-\alpha)\beta b'_y + \alpha\beta c'_y \end{aligned} \quad (8)$$

Where a'_x, b'_x, c'_x and a'_y, b'_y, c'_y are the coordinates of points a', b', c'.

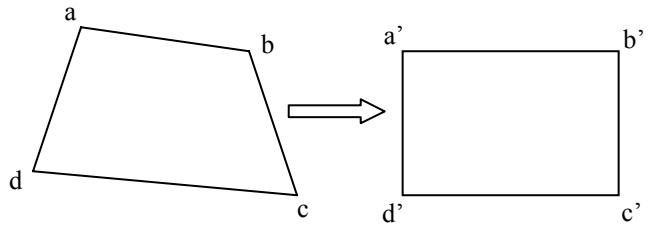

Figure 4. Mapping irregular quadrilateral to rectangle.

(3) Obtain three velocity values v_1, v_2, v_3 of three projected target points respectively in Plane(*x, y*), Plane(*z, y*) and Plane(*x, z*) using bilinear interpolation algorithm.

(4) Given (θ, σ, γ) as three angles between the vector of the target point and three planes, the velocity v of the target point is given as:

$$v = \sin^2\theta \cdot v_1 + \sin^2\sigma \cdot v_2 + \sin^2\gamma \cdot v_3 \quad (9)$$

III. Results and Discussion

A. Data Acquisition

All DTV data in our experiments were acquired using a GE Vivid7 ultrasound scanner with a M3S transducer. The 3D ultrasound data for the creation of 3D LV model is obtained using a Phillips IEE3 ultrasound scanner. Four sets of DTV images were acquired, where two sets were obtained from two healthy individuals respectively, other two sets were obtained from one patient before and after the DDD (Dual Mode) pacemaker implantation. The purpose is to compare the myocardial motion function between healthy individuals and patients, and the myocardial motion function of the same patient before and after pacemaker implantation. DDD pacemaker is an artificial pacemaker that can sense and pace both the atria and ventricles. In addition, gray Echo-cardiogram images were also acquired from all the test individuals, as reference for anatomical structures.

B. Evaluation of Registration

In this experiment, several similarity measures between floating images and reference images are calculated to illustrate the feasibility of our proposed registration methods, including Brightness Histogram Similarity (BHS), Color Histogram Similarity (CHS), Shape Histogram Similarity (SHS) and Feature Vector Similarity (FVS) [17]. Two images are more similar when the similarity value is bigger (Maximum value is equal to 1 for all measures).

Figure 5 shows nine Regions of Interest (ROI) segmented from the DTV images and the corresponding results mapped to the 3D LV model based on our proposed two-step registration methods.

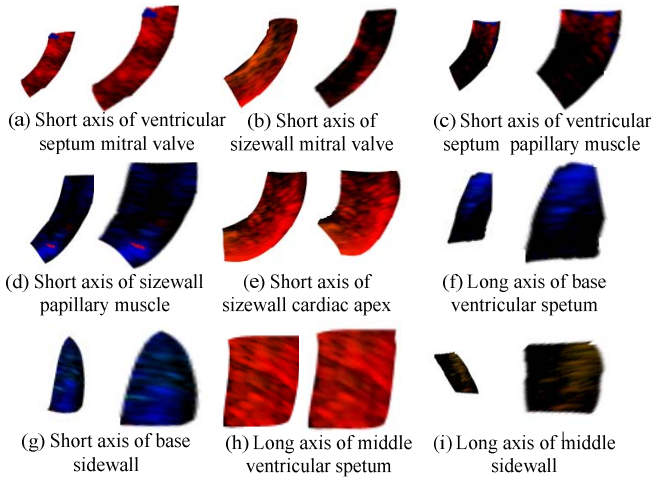

Figure 5. Left for each set: ROI segmented from DTV images; Right for each set: Result mapped to starntard model

The similarity results of above nine sets of images are shown in Table I. The mean of all the measures is bigger than 0.9. Image (a) achieves the best similarity. The high similarity between floating images and reference images illustrated promising feasibility of our proposed registration methods.

TABLE I. SIMILARITY MEASURE OF REGISTRATION.

	BHS	CHS	SHS	FVS	Average
Image a	0.986	0.972	0.958	0.952	0.967
Image b	0.997	0.960	0.938	0.966	0.965
Image c	0.984	0.856	0.832	0.825	0.874
Image d	0.980	0.963	0.932	0.920	0.949
Image e	0.990	0.928	0.915	0.941	0.944
Image f	0.985	0.930	0.940	0.932	0.947
Image g	0.987	0.955	0.80	0.783	0.881
Image h	0.996	0.940	0.910	0.920	0.942
Image i	0.995	0.910	0.740	0.911	0.889

C. *Comparison of Myocardial Motion Function between Healthy Individuals and Patients*

The motion of base segment, ventricular septum and sidewall of LV can effectively indicate the local systolic and diastolic function of LV. To the end, the velocity mapping of the third, sixth segment, the LV septum and sidewall is mainly studied and illustrated in this paper.

Figure 6 shows the myocardial velocity mapping to the LV model of one healthy individual. These images illustrate that the LV myocardial velocity of the healthy individual in the same phase has the live and uniform color. The color is red in the end-systolic phase and blue in the end-diastolic phase.

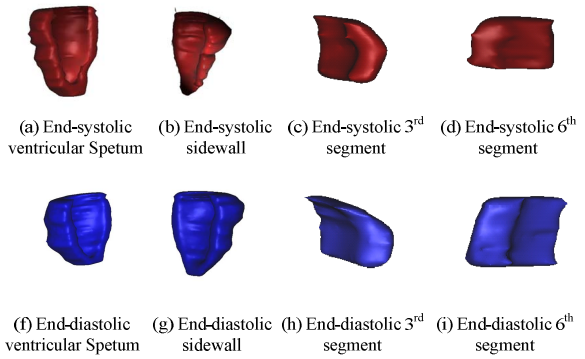

Figure 6. Velocity mapping of one healthy individual.

The results of the myocardial velocity mapping to LV model of one patient before and after the pacemaker implanted are displayed respectively in Figure 7 and 8. The color distribution before operation is not uniform and mixed with other colors, which indicates that abnormal myocardial motions exist in the cardio of the patient. While, the color distribution after the pacemaker implanted is similar to the healthy individual's, which indicates that the cardiac function of the patient is improved after operation.

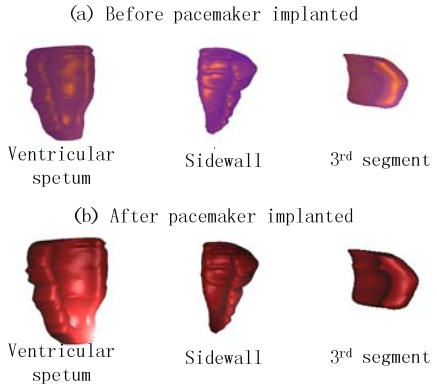

Figure 7. Velocity mapping of one patient in end-systolic phase, before and after the pacemaker was implanted respectively.

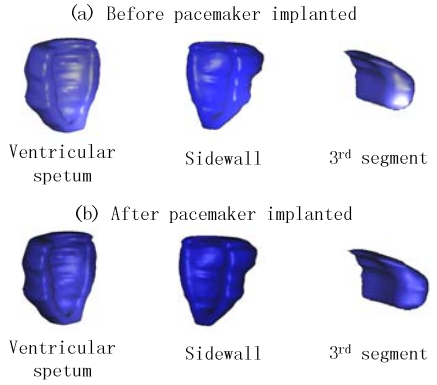

Figure 8. Velocity mapping of one patient in end-diastolic phase, before and after the pacemaker was implanted respectively.

IV. CONCLUSION

In this paper, we have proposed to build a 3D mechanical motion model of Left LV, in order to evaluate the paced myocardial function. Velocity information is mapped to 3D standard LV model based on our proposed two-step registration of DTV images and LV model. We also propose to adopt the fast interpolation method to map the velocity from multiple 2D images to 3D model. The preliminary experiments have shown promising feasibility of our methods. In the future, we will develop automatic algorithm to obtain the 16 segments from ultrasound images. We will further improve the motion mapping by replacing color information with other quantitative representatives. The long-term goal should be to develop a fully automatic algorithm to help the optimization of the pacing models.

ACKNOWLEDGMENT

This work described in this paper was fully supported by the National Natural Science Foundation of China (Nos. 60772147 and 60871060).

REFERENCES

[1] Kim WY, Sogaard P, et al, "Three Dimensional Echocardiography Documents Haemo dynamic Improvement by Biventricular Pacing in Patients with Severe Heart Failure", in Heart 2001, vol. 85, pp. 514-520.

[2] Kerwin WF, Botvinich EH,et al, "Ventricular Contraction Abnormalities in Dilated Cardiomyopathy: Effect of Biventricular Pacing to Correct Interventricular Dyssychrony", in J Am Coll Cardiol, 2000, vol. 35, pp. 1221-1227.

[3] Alonso C, Leclercq C, et al., "Electrocardiographic Predictive Factors of long-term Clinical Improvement with Multisite Biventricular Pacing in Advanced Heart Failure", in Am J Cardiol, 1999, vol. 84, pp. 1417-1421.

[4] Rouleau FDR, Merheb M, et al., "Echocardiographic Assessment of the Interventricular Delay of Activation and Correlation to the QRS Width in Dilated Cardiomyopathy", in PACE 2001, vol. 24, pp. 1500-1506.

[5] Frédéric Devernay and Eve Coste-Manière, "Three-Dimensional Motion Tracking of Coronary Arteries in Biplane Cineangiograms", in IEEE Trans Med Imaging, 2003, vol. 22(4), pp. 493-503.

[6] M. J. Ledesma-Carbayo, P. Mahia-Casado, A. Santos, E. Perez-David, M.A. Garcia-Fernandez and M. Desco, "Cardiac Motion Analysis From Ultrasound Sequences Using Nonrigid Registration: Validation Against Doppler Tissue Velocity", in Ultrasound in Med. & Biol, 2006, vol. 32(4), pp. 483-490.

[7] Suinesiaputra A, Frangi AF, Kaandorp TA, Lamb HJ, Bax JJ, Reiber JH, and Lelieveldt BP, "Automated Detection of Regional Wall Motion Abnormalities Based on a Statistical Model Applied to Multislice Short-axis Cardiac MR Images", in IEEE Trans Med Imaging, 2009, vol. 28(4), pp. 595-607.

[8] Nobuaki Yutaka, Nishi Toshifumi, Amano Akira and Matsuda Tetsuya, "Simulation Algorithm of Left Ventricular Mechanical Model for Coupling with Circulation Model", in Proceedings of the Annual Conference of the Institute of Systems, Control and Information Engineers, Japan, 2005, vol. 49, pp. 239-240.

[9] Han Hai-Chao, "An Echocardiogram-based 16-segment Model for Predicting Left Ventricular Ejection Fraction Improvement", in Journal of Theoretical Biology, 2004, vol. 228, pp. 7-15.

[10] Linninger, Andreas A., Michalis Xenos, Srinivasa Kondapalli, and Mahadevabharath R. Somayaji, "Mimics Image Reconstruction for Computer-Assisted Brain Analysis". Mimics, 2005.

[11] Penney, G., Blackall, J., Hamady, M., Sabharwal, T., Adam, A., Hawkes, D., "Registration of Freehand 3d Ultrasound and Magnetic Resonance Liver Images", in Medical Image Analysis, 2004, vol. 8, pp. 81-91.

[12] Bulow H, Dooley L and Wermser D, "Application of Principal Axes for Registration of NMR Image Sequences", in Pattern Recognition Letters, 2000, vol. 21, pp. 329-336.

[13] Jasper A. Vrugt, Hoshin V. Gupta, Willem Bouten and Soroosh Sorooshian, "A Shuffled Complex Evolution Metropolis algorithm for Optimization and Uncertainty Assessment of Hydrologic Model Parameters", in Water Resource Research, 2003, vol. 39, pp. 1201-1216.

[14] Ritter N, Owens R, Cooper J, Eikelboom RH, Van Saarloos PP, "Registration of Stereo and Temporal Images of the Retina", in IEEE Trans Med Imaging, 1999, vol. 18(5), pp. 404-418.

[15] Bookstein FL. Morphometric Tools for Landmark Data: Geometry and Biology. Cambridge University Press, 1991.

[16] Chen Baoping, Zhao Junlan, Yin Zhiling, "A Fast Approach to Realize Bilinear Interpolation Algorithm", in Journal of Beijing Electronic Science and Technology Institute, vol. 12(4), pp. 21-23.

[17] Linda G. Shapiro and George C. Stockman, Computer Vision, 2001, Prentice Hall.